[CANCER RESEARCH 63, 5513–5520, September 1, 2003]

# Dicumarol Inhibition of NADPH:Quinone Oxidoreductase Induces Growth Inhibition of Pancreatic Cancer via a Superoxide-mediated Mechanism[1]

**Joseph J. Cullen,[2] Marilyn M. Hinkhouse, Matthew Grady, Andrew W. Gaut, Jingru Liu, Yu Ping Zhang, Christine J. Darby Weydert, Frederick E. Domann, and Larry W. Oberley**

*Departments of Surgery [J. J. C.], Radiation Oncology [J. J. C., A. W. G., J. L., Y. P. Z., C. J. D. W., F. E. D., L. W. O.], and the Holden Comprehensive Cancer Center [J. J. C., F. E. D., L. W. O.], University of Iowa College of Medicine [M. G.], Iowa City, IA, and Veterans Affairs Medical Center [J. J. C., M. M. H.], Iowa City, Iowa 52242*

## ABSTRACT

**NADPH:quinone oxidoreductase ($NQO_1$), a homodimeric, ubiquitous, flavoprotein, catalyzes the two-electron reduction of quinones to hydroquinones. This reaction prevents the one-electron reduction of quinones by cytochrome P450 reductase and other flavoproteins that would result in oxidative cycling with generation of superoxide ($O_2^{\cdot-}$). $NQO_1$ gene regulation may be up-regulated in some tumors to accommodate the needs of rapidly metabolizing cells to regenerate $NAD^+$. We hypothesized that pancreatic cancer cells would exhibit high levels of this enzyme, and inhibiting it would suppress the malignant phenotype. Reverse transcription-PCR, Western blots, and activity assays demonstrated that $NQO_1$ was up-regulated in the pancreatic cancer cell lines tested but present in very low amounts in the normal human pancreas. To determine whether inhibition of $NQO_1$ would alter the malignant phenotype, MIA PaCa-2 pancreatic cancer cells were treated with a selective inhibitor of $NQO_1$, dicumarol. Dicumarol increased intracellular production of $O_2^{\cdot-}$, as measured by hydroethidine staining, and inhibited cell growth. Both of these effects were blunted with infection of an adenoviral vector containing the cDNA for manganese superoxide dismutase. Dicumarol also inhibited cell growth, plating efficiency, and growth in soft agar. We conclude that inhibition of $NQO_1$ increases intracellular $O_2^{\cdot-}$ production and inhibits the *in vitro* malignant phenotype of pancreatic cancer. These mechanisms suggest that altering the intracellular redox environment of pancreatic cancer cells may inhibit growth and delineate a potential strategy directed against pancreatic cancer.**

## INTRODUCTION

Pancreatic cancer is one of the most aggressive malignancies, the fourth leading cause of cancer death in the United States, and increasing in incidence (1). Surgical resection of the primary tumor remains the only potentially curative treatment for pancreatic cancer; however, in population-based studies the number of patients undergoing resection with curative intent can be <3% (2). Even after resection, median survival is only 12–18 months, and <20% of resected patients survive 5 years and the majority die of metastatic cancer recurrence (3). Other adjuvant treatments such as radiation therapy and chemotherapy have not improved long-term survival after resection. The rate of chemotherapeutic response is <20% (4), whereas <10% of patients benefit from radiation therapy (5, 6). Because of the lack of poor therapeutic responsiveness of pancreatic cancer to surgery, chemotherapy, and radiation therapy, survival beyond 5 years is rare with the median survival <6 months (3). Thus, effective therapies for pancreatic cancer are needed to control progression and metastatic disease.

$NQO_1$[3] (DT-diaphorase; EC 1.6.99.2), a homodimeric, ubiquitous, cytosolic, and membrane flavoprotein, is considered to be a deactivation enzyme, because it catalyzes the two-electron reduction of quinones, including membrane ubiquinone (7). This reaction prevents the one-electron reduction of quinones by cytochrome P450 reductase and other flavoproteins that would redox cycle with molecular oxygen to generate $O_2^{\cdot-}$. $NQO_1$ has been shown to redox, couple with, and reduce membrane ubiquinone, and both quinone reductase activity and ubiquinone have been established previously as necessary for function of the plasma membrane electron transport system (8). $NQO_1$ also plays a role as an antioxidant enzyme, and generates antioxidant forms of ubiquinone and $\alpha$-tocopherol during oxidative stress (9, 10). As a result of its protective effects, $NQO_1$ has been proposed to function as a chemopreventive enzyme (11–13). However, $NQO_1$ may also catalyze bioactivation of antitumor quinones (14–16) and is expressed at high levels in many solid tumors including pancreatic cancer (17–19). A recent study by Logsdon *et al.* (19) using microarrays demonstrated that there is a 10-fold up-regulation of $NQO_1$ in pancreatic cancer when compared with normal pancreas. The $NQO_1$ properties of catalyzing bioactivation of antitumor quinones and high expression in pancreatic cancer make it a principal target in therapeutic strategies to design chemotherapeutic agents.

Like other flavoenzymes, $NQO_1$ is inhibited by DPI and the quinone analogue capsaicin (20). It differs from other quinone reductases in the cell in that it uses both NADH and NADPH as cofactors, and is selectively inhibited by low concentrations of dicumarol (21). $NQO_1$ gene regulation is greatly up-regulated in various solid tumors compared with normal tissues of the same origin, perhaps to accommodate the needs of rapidly metabolizing cells to regenerate $NAD^+$ (22).

Because pancreatic cancer is one of the most aggressive malignancies with rapid turnover and short doubling times, we hypothesized that pancreatic cancer cells would exhibit high levels of $NQO_1$, and inhibiting it would suppress the malignant phenotype. Our study demonstrates that $NQO_1$ is up-regulated in pancreatic cancer cell lines. Inhibition of $NQO_1$ with dicumarol increased intracellular $O_2^{\cdot-}$ and inhibited the *in vitro* malignant phenotype of pancreatic cancer. The effect of inhibiting cell growth by dicumarol may be because of increased intracellular $O_2^{\cdot-}$ production, because enforced expression of MnSOD decreased hydroethidine staining and reversed the inhibition of cell growth.

## MATERIALS AND METHODS

### Human Pancreas

Human pancreatic specimens were retrieved from neurologically devastated, heart-beating patients that were transplant donors where the pancreas was considered unsuitable for transplantation or no recipient was available. Pancreatic specimens were discarded and not used in this study if the donor had any history of pancreatic disease. All of the specimens were retrieved at the University of Iowa Hospitals and Clinics. The protocol to use the human pancreatic specimens was approved by the University of Iowa Institutional Review Board for Human Subjects on February 12, 2001.

Received 4/10/03; revised 6/12/03; accepted 6/20/03.

The costs of publication of this article were defrayed in part by the payment of page charges. This article must therefore be hereby marked *advertisement* in accordance with 18 U.S.C. Section 1734 solely to indicate this fact.

[1] Supported by NIH Grants DK 60618, CA 66081, and the Medical Research Service, Department of Veterans Affairs.

[2] To whom requests for reprints should be addressed at 4605 JCP, University of Iowa Hospitals and Clinics, Iowa City, IA 52242. Phone: (319) 353-8297; Fax: (319) 356-8378; E-mail: joseph-cullen@uiowa.edu.

[3] The abbreviations used are: $NQO_1$, NADPH:quinone oxidoreductase; DPI, diphenylene iodonium; Mn, manganese; SOD, superoxide dismutase; RT-PCR, reverse transcription-PCR; Ad*MnSOD*, adenovirus-*MnSOD* construct; MOI, multiplicity of infection.

### Cell Culture

The following human pancreatic adenocarcinoma cell lines were obtained from American Type Culture Collection (Manassas, VA): BxPC-3 (poorly differentiated), Capan-1 (moderately to well differentiated), MIAPaCa-2 (undifferentiated), and AsPC-1 (poorly to moderately differentiated). BxPC-3 was maintained in RPMI 1640 with 10% fetal bovine serum. Capan-1 was maintained in Iscove's modified Dulbecco's medium with 20% fetal bovine serum. MIA PaCa-2 was maintained in DMEM supplemented with 10% heat-inactivated fetal bovine serum and 2.5% horse serum. AsPC-1 was maintained in RPMI 1640 with 20% heat-inactivated bovine serum and 1% sodium pyruvate. All of the media was obtained from Life Technologies, Inc. (Grand Island, NY) and all of the cell lines were maintained at 37°C.

### RT-PCR for Detection of $NQO_1$ mRNA

For RT-PCR detection of $NQO_1$, PCR was performed using the $NQO_1$-specific primers 5′-CAGCGCCCCGGACTGCACCAGAGCC and -3′-GGGAAGCCTGGAAA-GATACCCAGA (24). PCR was continued for 30 cycles under the following conditions: denaturation at 94°C for 60 s, annealing at 58°C for 60 s, and elongation at 72°C for 120 s on cycles 1–29 and 10 min on cycle 30. $\beta$-Actin was used as a control for RNA input. Bands were stained with ethidium bromide and photographed under UV light. Sequence identity of RT-PCR products was confirmed by gel purification and sequencing by the University of Iowa DNA Facility.

**Cell Homogenization and Protein Determination.** Cells were washed three times in PBS (pH 7.0), scraped from the dishes using a rubber policeman, and then collected in potassium phosphate buffer (pH 7.8). This was followed by sonic disruption on ice for 30 s in 10-s bursts using a VibraCell sonicator (Sonics and Materials Inc., Danbury, CT) at 100% power. Protein concentration was determined using the Bio-Rad Bradford dye binding protein assay kit (Hercules, CA) according to the manufacturer's instructions.

### Western Blot Analysis for $NQO_1$ Protein

The $NQO_1$ monoclonal antibodies were kindly supplied by Dr. David Ross (University of Colorado Health Science Center, Denver, CO). Total protein extracts were prepared and protein concentrations determined. Protein (20 $\mu$g/lane) was separated by 12% SDS-PAGE and electrotransferred to nitrocellulose membranes. After transfer, membranes were blocked with Tris-buffered saline containing 5% skim milk powder and 1% heat-inactivated fetal bovine serum for 2 h, and then incubated overnight with the anti-$NQO_1$ monoclonal antibody (1:100) at 4°C. Blots were washed in Tris-buffered saline containing 0.05% Tween 20 and incubated for 90 min with 1:4000 dilution of goat antimouse horseradish peroxidase-conjugated antibody in Tris-buffered saline containing 1% skim milk powder and 1% heat-inactivated fetal bovine serum. Bands were visualized using an enhanced chemiluminescence detection kit (Amersham Life Science, Buckinghamshire, United Kingdom) and exposed to X-ray film as described previously (23).

### $NQO_1$ Activity Assay

An indirect, coupled assay was used to measure $NQO_1$ activity in the normal pancreas, pancreatic cancer cell lines, and in the MIA PaCa-2 cell line after 4 h of treatment with dicumarol (0–250 $\mu$M). Cells were harvested by scraping and frozen at −80°C. Cell extracts were suspended in 0.45 ml PBS plus 50 $\mu$l of a 10% solution of aprotinin and sonicated by exposure to five 10-s ultrasound pulses using a Vibra Cell sonicator. Activity was assayed spectrophotometrically by measuring cytochrome *c* reduction at 550 nm in the presence of NADH as described by Fitzsimmons *et al.* (25). Standard reaction mixtures (1 ml) contained cytochrome *c* (77 $\mu$M), NADH (cofactor, 200 $\mu$M), menadione (intermediate electron acceptor; 10 $\mu$M), BSA (0.14%), and Tris-HCl buffer (50 mM; pH 7.5). The activity attributable to $NQO_1$ activity in the cell extracts was that which was inhibited by dicumarol (10 $\mu$M). All of the reactions were carried out at 37°C, rates of reduction were calculated from the initial linear part of the reaction curves, and units of enzyme activity were expressed as nanomoles of cytochrome *c* reduced per minute per milligram of protein. An extinction coefficient for cytochrome *c* of 21.1 mM/cm was used in the calculations.

### *In Vitro* Growth Characteristics

**Cell Growth.** Cells ($1 \times 10^4$) were plated in triplicate in 1.5 ml complete medium in 24-well plates. Cells were trypsinized and then counted on alternate days for 2 weeks using a hemocytometer. Cell population doubling time in hours (*DT*) was determined in triplicate using the following equation:

$$DT(\text{h}) = 0.693(t - t_o)/\ln(N_t/N_o)$$

where $t_o$ = time at which exponential growth began, $t$ = time in hours, $N_t$ = cell number at time $t$, and $N_o$ = initial cell number (26). To determine the role of $NQO_1$ inhibition, dicumarol (50–250 $\mu$M) was added to MIA PaCa-2 cell cultures. A 50 mM concentration of dicumarol was dissolved in water by drop-wise addition of 0.1 *n* NaOH. Addition of up to 2.5 $\mu$l of this solution per ml (250 $\mu$M highest final concentration) did not change the pH of complete medium.

**Plating Efficiency.** Control and dicumarol-treated cells ($2 \times 10^3$) were plated in triplicate into 60-mm dishes in complete medium. The dishes were maintained in the incubator for 6 days to allow colony formation. The colonies were then fixed and stained with 0.1% crystal violet and 2.1% citric acid, and those colonies containing >50 cells were scored.

**Anchorage-independent Growth in Soft Agar.** Cells ($5 \times 10^3$) were suspended in 3 ml of complete medium containing dicumarol (0–250 $\mu$M) in a solution of 6% agar in double-distilled $H_2O$ so that the final concentration of the agar was 0.3%. This suspension was then plated over 3 ml of complete medium made using a 6% agar solution in double-distilled $H_2O$ so that the final concentration of the bottom agar was 0.5%. After 16 days, colonies of >0.1 mm in diameter were scored. The clonogenic fraction was determined using the following equation:

$$\text{Soft Agar Plating Efficiency (PE)} = (\text{colonies formed/cells seeded}) \times 100.$$

### Determination of Reactive Oxygen Species

To dissect potential sources of $O_2^{\cdot-}$ production the following inhibitors of major oxidases were added: the $NQO_1$ inhibitor dicumarol (50–250 $\mu$M), the flavoprotein inhibitor DPI (100 $\mu$M), and an Ad*MnSOD*. $O_2^{\cdot-}$ production was determined using three different assays.

**Lucigenin Assay.** Production of $O_2^{\cdot-}$ was measured by lucigenin-enhanced chemiluminescence. Cells were placed in a microplate well containing PBS and placed in a microplate luminometer. Lucigenin (5 $\mu$M to avoid superoxide production) was added by injector, mixed by orbital shaker, and luminescence measurements obtained every 30 s for 10 min at 37°C. The luminometer reports relative light units emitted, which are proportional to superoxide levels. Dark current readings (photomultiplier background signal) were subtracted. The maximum rate of superoxide generation and the integrated relative light units for 10 min was determined and normalized to mg of protein. An advantage of using the microplate system for measurement of superoxide levels in cells is that the measurement can be made in attached cells (which may have differences from cells in suspension), and there is no need for digestion from the culture plate to obtain a cell suspension (which may alter cell function).

**Hydroethidine.** Intracellular generation of $O_2^{\cdot-}$ was assessed using hydroethidine fluorescence. $O_2^{\cdot-}$ reacts with hydroethidine to produce ethidium bromide, which binds to nuclear DNA and fluoresces red. Hydroethidine is one of the best reagents now available for measuring intracellular $O_2^{\cdot-}$. Cells were incubated for 30 min with hydroethidine (5 $\mu$M) and after rinsing to remove extracellular dye, fluorescence was detected in the cells with a Bio-Rad MRC-1024 laser scanning confocal microscope equipped with a krypton-argon laser. Excitation and emission wavelengths were 488 and 610 nm. Fluorescence was detected with a 585-nm long pass filter. Control and treatment groups were always imaged in parallel to ensure that the processing techniques and laser settings were identical. All of the images were collected using a $512 \times 512$ pixel format and archived for subsequent analysis. The fluorescence of hydroethidine was quantitated using flow cytometry. Cells were grown to subconfluence in 60-mm dishes, and initially treated with or without dicumarol (50–250 $\mu$M) for 4 h, washed, and incubated with hydroethidine (10 $\mu$M) for 40 min. The cells were removed by trypsinization, which was neutralized with PBS containing 10% FCS and then analyzed by flow cytometry (Becton Dickinson FACScan). To determine the specificity of $O_2^{\cdot-}$ changes with

dicumarol treatment, subsequent experiments were performed with cells receiving no treatment (controls), dicumarol 100 $\mu$M, or dicumarol 100 $\mu$M + pretreatment with an adenoviral construct containing the cDNA for MnSOD.

**Cytochrome *c*.** Unfortunately, in live cells, the cytochrome *c* assay can only measure extracellular $O_2^{\cdot -}$ and that is why the above assays are useful, even if they may not be as specific. The cytochrome *c* assay relies on the use of the addition of SOD to make it specific for $O_2^{\cdot -}$. For this assay one simply follows the reduction of cytochrome *c* spectrophotometrically at 550 nm in the absence and presence of SOD protein. An extinction coefficient of $\Delta E_{M550\ nm} = 2.1 \times 10^4\ M^{-1}cm^{-1}$ was used to calculate $O_2^{\cdot -}$ levels.

**Adenovirus Gene Transfer.** To determine the specificity of the above assays in measuring $O_2^{\cdot -}$ generation and to delineate the mechanisms of $NQO_1$ inhibition on pancreatic tumor cell growth, additional experiments were performed on MIA PaCa-2 cells by increasing expression of MnSOD using an adenoviral vector containing the cDNA for MnSOD. The adenovirus construct used was a replication-defective, E1- and partial E3-deleted recombinant adenovirus (26). Inserted into the E1 region of the adenovirus genome is the human *MnSOD* gene, which is driven by a cytomegalovirus promoter. The adenovirus construct was obtained from the University of Iowa Gene Transfer Vector Core.

Approximately $10^6$ MIA PaCa-2 were plated in 10 ml of complete medium in a 90-$cm^2$ plastic dish and allowed to attach for 24 h. Cells were then washed three times in serum- and antibiotic-free medium. The Ad*MnSOD*, suspended in 3% sucrose, was then applied to cells suspended in 4 ml of serum- and antibiotic-free medium at 100 MOI. Cells were incubated with the adenovirus constructs for 24 h. Medium was then replaced with 4 ml of complete medium for an additional 24 h before cells were harvested. Three days later, intracellular generation of $O_2^{\cdot -}$ was assessed using hydroethidine fluorescence and cell growth curves determined in MIA PaCa-2 cells (controls), MIA PaCa-2 cells treated with dicumarol (100 $\mu$M) for 4 h, and MIA PaCa-2 cells infected with Ad*MnSOD* and then treated with dicumarol (100 $\mu$M) for 4 h. Also, cells were harvested to determine changes in MnSOD protein and activity after infections with and without Ad*MnSOD*. Immunoreactive protein corresponding to MnSOD was identified and quantitated from total cell protein by the specific reaction of the immobilized protein with its antibody. Total protein was electrophoresed in a 12.5% SDS-polyacrylamide running gel and a 5% stacking gel. The proteins were then electrotransferred to nitrocellulose sheets. After blocking in 20% fetal bovine serum for 1 h, the sheets were washed and then treated with antisera to MnSOD (1:1000) for 1 h. Polyclonal rabbit-antihuman antibodies to MnSOD has been prepared and characterized in our laboratory (27). This antibody has been shown to react with the appropriate protein in a variety of species, including hamster (28) and human (23, 26). The blot was incubated with horseradish peroxidase-conjugated goat-antirabbit



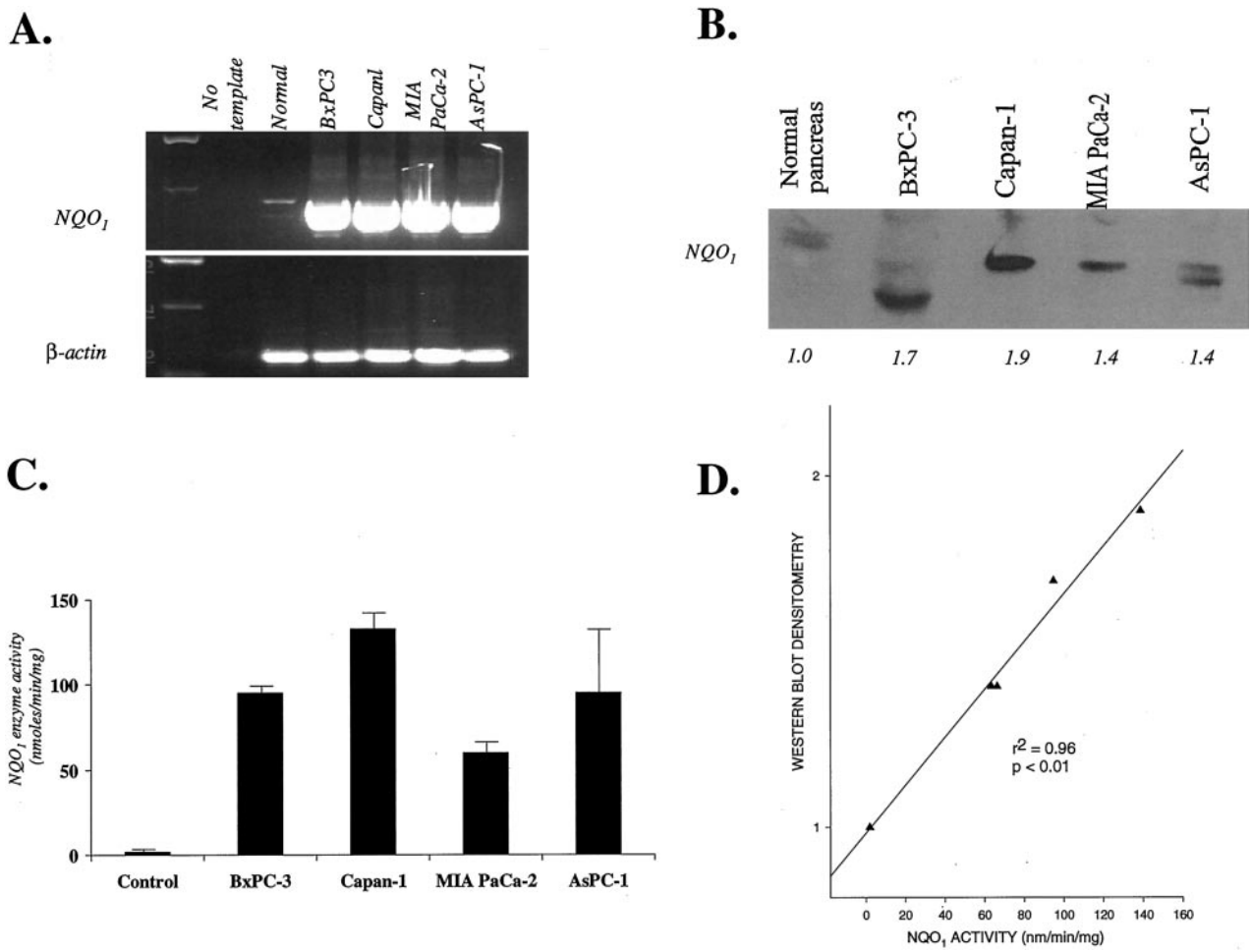


Fig. 1. *A*, $NQO_1$ is expressed to high levels in pancreatic cancer cell lines but not in normal human pancreas. RNA was harvested and semiquantitative RT-PCR performed for $NQO_1$. Primers used were sense: 5′-CAGGCGCCCCGGACTGCACCAGAGCC and antisense: 3′-GGGAAGCCT-GGAAAGA-TACCCAGA. Reaction products were resolved and visualized on a 1% agarose gel. Sequence identity of RT-PCR products was confirmed by gel purification and sequencing by the University of Iowa DNA Facility. $\beta$-Actin was used as a control for RNA input. *B*, $NQO_1$ protein is expressed at elevated levels in pancreatic carcinoma cells compared with normal pancreas. Total protein extracts were prepared and protein concentrations determined. Protein (20 $\mu$g/lane) was separated by 12% SDS-PAGE and electrotransferred to nitrocellulose membranes. After transfer, membranes were blocked and then incubated overnight with anti-$NQO_1$ monoclonal antibody. The area of the bands relative to the human pancreas cells as measured by densitometric analysis is shown at the *bottom of the lanes*; these numbers indicate the relative amount of immunoreactive protein. *C*, $NQO_1$ enzymatic activities are increased in pancreatic cancer cell lines compared with normal pancreas. Activity was assayed spectrophotometrically by measuring cytochrome *c* reduction at 550 nm in the presence of NADH. *Bars*, $\pm$SE; $n = 3$. *D*, correlation plots of $NQO_1$ immunoreactive protein densitometry *versus* $NQO_1$ enzymatic activity. Enzymatic activity and the Western blot were determined from the same sample. Immunoreactivity for $NQO_1$ protein correlated well ($r^2 = 0.96$; $P < 0.01$) with the $NQO_1$ activity assay.

(Sigma) IgG (1:10,000) for 1 h at room temperature. The washed blot was then treated with enhanced chemiluminescence Western blot detection solution (Amersham Life Science) and exposed to X-ray film.

## RESULTS

**RT-PCR for Detection of $NQO_1$ mRNA.** RT-PCR demonstrated that $NQO_1$ is expressed in four human pancreatic cancer cell lines. Fig. 1*A* shows that the $NQO_1$ PCR bands are much more intense in the pancreatic cancer cell lines than in normal human pancreas as reported in other solid tumors when compared with normal cells of the same origin (25).

**Western Analysis for $NQO_1$.** The levels of $NQO_1$ immunoreactive protein expressed in human pancreas and pancreatic cancer cell lines were assessed by Western blot analysis. Fig. 1*B* demonstrates immunoreactive protein for $NQO_1$. Normal human pancreas had minimal amounts of immunoreactive protein when compared with the four cell lines. In normal pancreas and the AsPC-1 cell line, two distinct bands could be seen in the Western analysis. Previous studies have suggested that the lower molecular weight band ($M_r$ 500–1000 smaller than wild-type $NQO_1$) observed may be a result of proteolytic processing or chemical degradation and was included in the densitometric analysis (29). It should be noted that the increases in $NQO_1$ mRNA shown in Fig. 1*A* appear to be greater than the increases in $NQO_1$ protein shown in Fig. 1*B*. This could be because the RT-PCR reaction was only semiquantitative and was saturated in the carcinoma samples after 30 cycles. The significance of the different migrations in the Western blots is unknown, but suggests that the proteins in the cancer cell lines may be different because of mutations or some other protein modification.

**$NQO_1$ Enzyme Activity.** Fig. 1*C* demonstrates $NQO_1$ enzyme activity, which was significantly higher in the pancreatic cancer cell lines when compared with normal pancreas. Normal pancreas had $NQO_1$ enzyme activity of 1.7 ± 0.3 nmol/min/mg compared with $NQO_1$ enzyme activity in the pancreatic cancer cell, lines, which ranged from 60 ± 4 nmol/min/mg in the MIA PaCa-2 cell line up to 133 ± 12 nmol/min/mg in the Capan-1 cell line.

To determine whether the $NQO_1$ activity assay correlated with the protein levels measured by the Western blot, we examined the relationship between two quantitative variables, activity and protein, using Pearson's correlation coefficient and linear regression. We harvested cells, and performed both the activity assay and a Western blot on the same cell homogenate. The $NQO_1$ enzyme activity assay correlated well ($r^2 = 0.96$; $P < 0.01$) with the results obtained with the $NQO_1$ immunoblot (Fig. 1*D*).

**Tumor Biological Characteristics of $NQO_1$-treated Cells.** Cell growth inhibition of $NQO_1$ with dicumarol slowed the *in vitro* growth of MIA PaCa-2 pancreatic cancer cells (Fig. 2*A*). MIA PaCa-2 cell doubling time significantly increased with dicumarol (50–250 μM) when compared with the parental cells. Tumor cell doubling time increased from 21.5 ± 0.2 h for the parental cell line to 22.5 ± 0.2, 28.1 ± 0.9, and −14.1 ± 1.5 h with 50, 100, and 250 μM dicumarol, respectively. For example, 48 h after dicumarol treatment, cell number decreased by ~37% with 100 μM dicumarol and by 81% with 250 μM dicumarol compared with the MIA PaCa-2 cells with no treatment (Fig. 2*A*).

**Plating Efficiency.** To determine the clonogenic capacity of dicumarol-treated cells, we performed a plating efficiency assay in the MIA PaCa-2 cell line. In general, malignant cells have a higher plating efficiency than do normal cells. Plating efficiency was reduced in the dicumarol-treated cells compared with the parental cells (Fig. 2*B*). Plating efficiency was 24.3 ± 2.3% in the untreated MIA PaCa-2 cells. Inhibition of $NQO_1$ with the higher doses of dicumarol (100 and 250 μM) significantly decreased the plating efficiency to 10.0 ± 0.6%, and to nondetectable levels, respectively ($P < 0.01$ *versus* control).

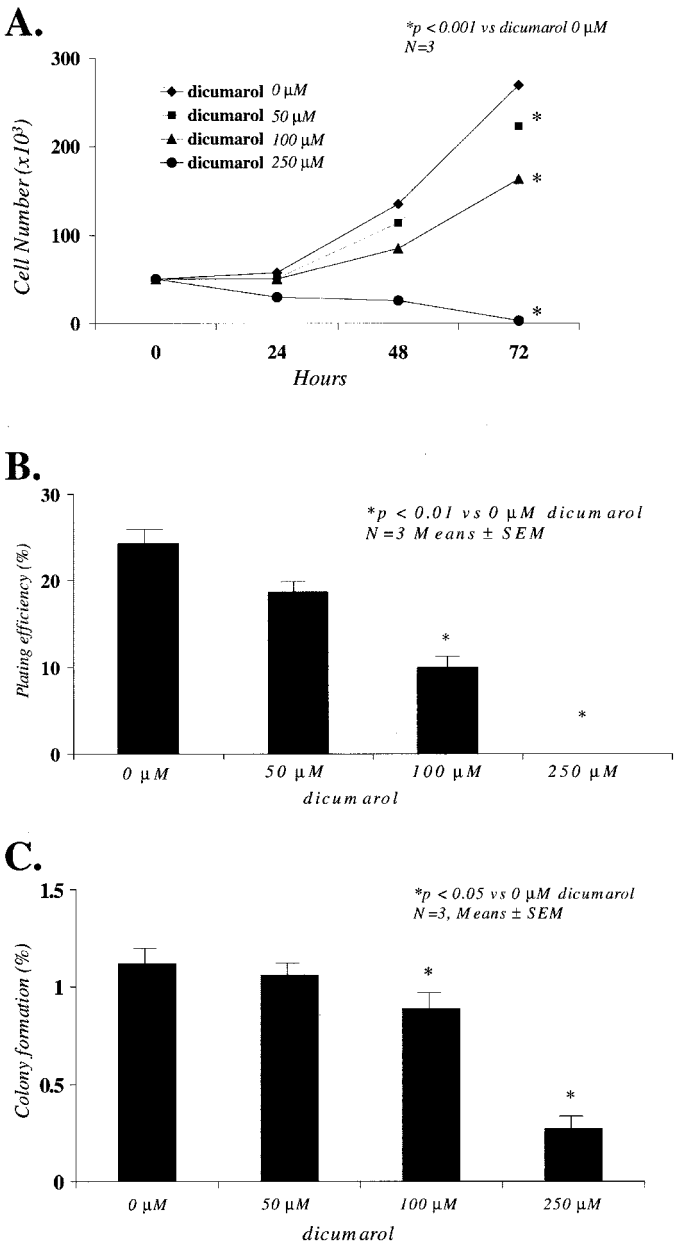


Fig. 2. Dicumarol inhibits the *in vitro* pancreatic cancer malignant phenotype. *A*, cell growth. MIA PaCa-2 cells treated with dicumarol (50, 100, and 250 μM) demonstrate reductions in cell growth. Each point was determined in triplicate from the same culture. *, $P < 0.001$ *versus* MIA PaCa-2 cells that received vehicle (*controls*). *B*, plating efficiency. MIA PaCa-2 cells treated with dicumarol (50, 100, and 250 μM) demonstrate reductions in plating efficiency. Mean plating efficiency of dicumarol (0–250 μM) MIA PaCa-2 cells are shown. Each determination was performed in triplicate from the same culture. $P < 0.01$ *versus* MIA PaCa-2 cells (*controls*). *C*, growth in soft agar. MIA PaCa-2 cells treated with dicumarol (50, 100, and 250 μM) demonstrate reductions in soft agar plating efficiency. Mean plating efficiency in soft agar of dicumarol (0–250 μM) MIA PaCa-2 cells are shown. Each determination was performed in triplicate from the same culture. *, $P < 0.05$ *versus* MIA PaCa-2 cells (controls).

**Growth in Soft Agar.** To examine anchorage-dependent growth, we performed a soft agar assay. Whereas malignant MIA PaCa-2 cells form colonies in soft agar, normal cells do so in far smaller numbers. As seen with plating efficiency, dicumarol significantly reduced colony formation (Fig. 2*C*) with the higher doses of dicumarol. Soft agar plating efficiency was 1.1 ± 0.1% in the parental cells and significantly reduced to 0.9 ± 0.1% in cells treated with dicumarol 100 μM.

Maximal reduction in colony formation was observed at a dicumarol dose of 250 $\mu$M, where the colony formation decreased to 0.3 $\pm$ 0.03% (Means $\pm$ SE; $P < 0.05$, 50, and 100 $\mu$M dicumarol-treated cells *versus* 0 $\mu$M dicumarol).

**Superoxide Production in Dicumarol-treated Cells.** To investigate whether inhibition of $NQO_1$ with dicumarol would alter generation of $O_2^{\cdot -}$, MIA PaCa-2 cells were treated with an inhibitor of flavoenzymes, DPI, and a selective inhibitor of $NQO_1$, dicumarol (0–250 $\mu$M), for 4 h. Cells were washed, and lucigenin-enhanced chemiluminescence was performed for detection of $O_2^{\cdot -}$. Neither DPI nor dicumarol had any effect on $O_2^{\cdot -}$ levels in MIA PaCa-2 cells (Fig. 3*A*) as measured by lucigenin-enhanced chemiluminescence. Additionally, dicumarol (100 and 250 $\mu$M) had no effect on $O_2^{\cdot -}$ levels measured by the cytochrome *c* assay (Fig. 3*B*). DPI (100 $\mu$M) caused a slight decrease in $O_2^{\cdot -}$ levels as measured by cytochrome *c* (MIA PaCa-2: 3.43 $\pm$ 0.08 nmol/$10^6$ cells/h *versus* DPI 100 $\mu$M: 2.81 $\pm$ 0.15 nmol/$10^6$ cells/h; $P < 0.05$ *versus* control; $n = 3$). Thus, DPI, which is a nonspecific inhibitor of NADPH oxidase, may have affected membrane oxidases that the cytochrome *c* could detect, whereas dicumarol did not.

Next, cells were treated with DPI (100 $\mu$M) and with dicumarol (50–250 $\mu$M) for 4 h, washed and incubated with hydroethidine, and examined with flow cytometry (Fig. 3*C*) and confocal laser scanning microscopy (Fig. 3*D*). Treatment with DPI resulted in a 2.2-fold increase in hydroethidine fluorescence as measured by flow cytometry. Treatment with dicumarol (50 and 100 $\mu$M) resulted in a 2.2- and 2.5-fold increase in hydroethidine fluorescence as measured by flow cytometry ($P < 0.05$ *versus* dicumarol $\mu$M; $n = 3$). Dicumarol (250 $\mu$M) had little effect on hydroethidine fluorescence when compared with no treatment. These differences may be explained in that higher doses of dicumarol are extremely toxic to the MIA PaCa-2 cell line leading to overwhelming cell death as evidence by the effects of this dose of dicumarol in the growth curves, soft agar, and plating efficiencies.

To determine whether the signal measured by hydroethidine fluorescence resulted from $O_2^{\cdot -}$, we used an Ad*MnSOD*. MIA PaCa-2 cells were incubated with the adenovirus constructs at 100 MOI for 24 h. Three days later, cells (infected and noninfected) were treated with dicumarol for 4 h, incubated with hydroethidine, and examined by flow cytometry and confocal laser scanning microscopy. An increase in MnSOD immunoreactivity was observed in cells infected with the Ad*MnSOD* construct and then treated with dicumarol (Fig. 4*A*). MnSOD immunoreactivity was low in the parental cells and in the dicumarol-treated cells. MIA PaCa-2 cells infected with Ad*MnSOD* blocked the increase in hydroethidine fluorescence seen with treatment by dicumarol (100 $\mu$M) when examined with flow cytometry (Fig. 4*B*) and confocal laser scanning microscopy (Fig. 4*C*).

To determine whether the increased $O_2^{\cdot -}$ levels from dicumarol treatment was leading to inhibition of cell growth in the MIA PaCa-2 cells, we performed growth curves on the parental cell line, MIA PaCa-2 cells without treatment without dicumarol (0 $\mu$M), treated with

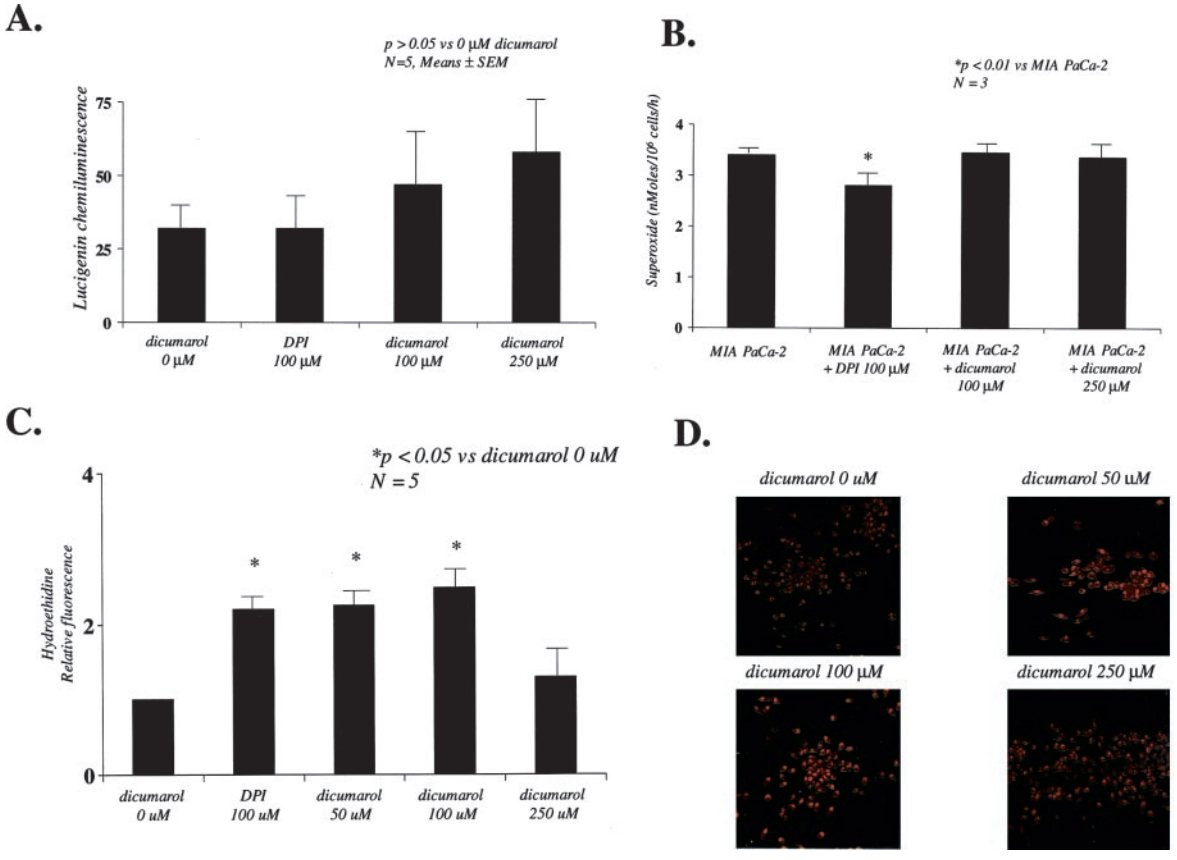


Fig. 3. DPI and dicumarol increased $O_2^{\cdot -}$ levels in MIA PaCa-2 cells as measured by hydroethidine fluorescence but not by lucigenin-enhanced chemiluminescence or cytochrome *c*. *A*, MIA PaCa-2 cells were exposed to DPI and dicumarol at the indicated concentrations, and 4 h later lucingenin-enhanced chemiluminescence was performed. Compared with the parental cell line, treatment of cells with DPI or dicumarol did not significantly change lucigenin-enhanced chemiluminescence. *B*, MIA PaCa-2 cells were exposed to DPI and dicumarol at the indicated concentrations, and 4 h later the cytochrome *c* assay was performed. DPI significantly decreased cytochrome *c* reduction; however, dicumarol (100 and 250 $\mu$M) had no effect. *C*, DPI and dicumarol increased intracellular $O_2^{\cdot -}$ levels as detected by hydroethidine fluorescence and flow cytometry. Cells were treated with DPI (100 $\mu$M) and dicumarol (50–250 $\mu$M) for 4 h. The cells were then incubated with hydroethidine (10 $\mu$M) and fluorescence quantitated by flow cytometry. *Bars*, $\pm$SE, $P < 0.05$ *versus* the parental cell lines (*controls*), $n = 3$. *D*, after incubation with hydroethidine, cells were also examined by confocal laser scanning microscopy. Hydroethidine is oxidized by $O_2^{\cdot -}$ and intercalates with DNA, yielding a bright red fluorescence.

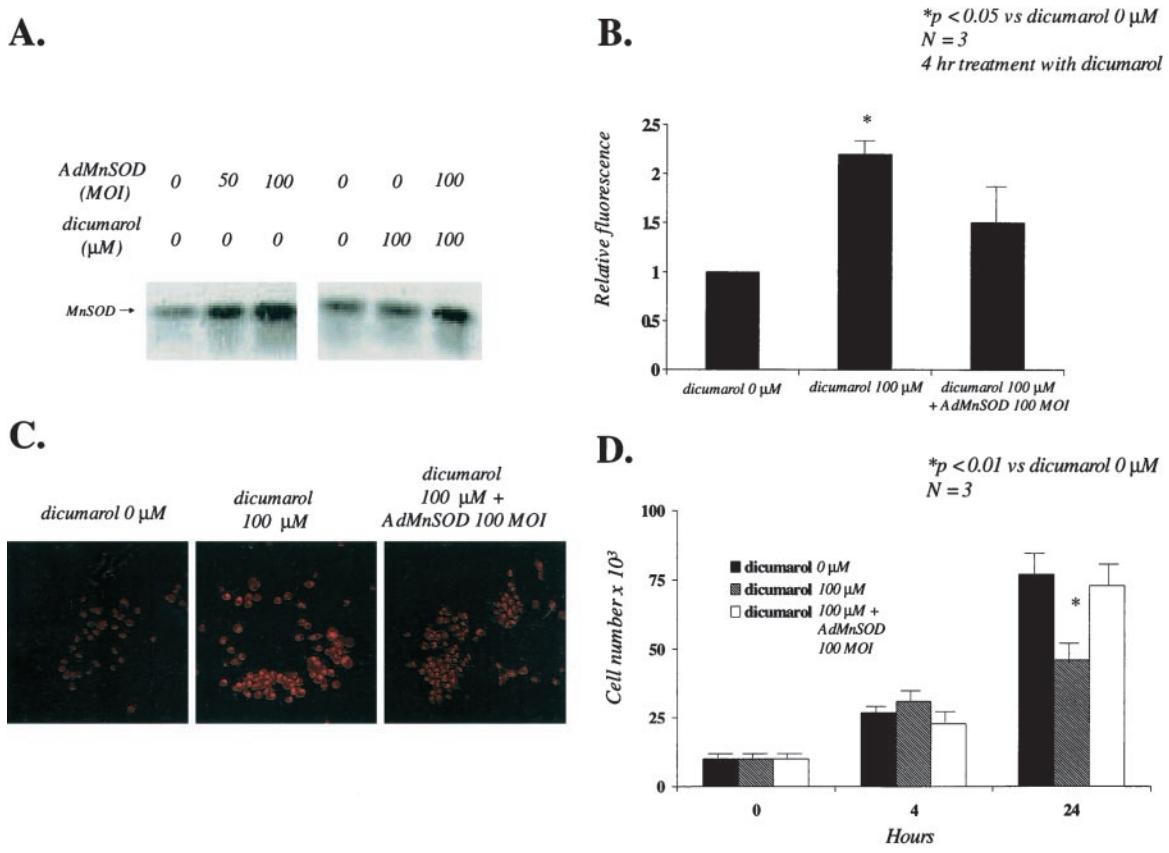


Fig. 4. *A,* MnSOD immunoreactive protein is increased after infection with Ad*MnSOD*. Increases in Ad*MnSOD* MOI increased MnSOD protein levels in MIA PaCa-2 cells. MIA PaCa-2 cells infected with 100 MOI Ad*MnSOD* and then treated with dicumarol (100 $\mu$M) demonstrate increases in MnSOD immunoreactivity compared with cells not infected with the adenoviral construct. MnSOD immunoreactivity was similar in the MIA PaCa-2 cells compared with MIA PaCa-2 cells treated with dicumarol (100 $\mu$M). *B,* dicumarol (100 $\mu$M) increased intracellular $O_2^{\cdot -}$ levels as detected by hydroethidine fluorescence and flow cytometry. Cells received no treatment, treatment with dicumarol (100 $\mu$M) for 4 h, and transfected with the Ad*MnSOD* vector and treatment with dicumarol (100 $\mu$M) for 4 h. The cells were then incubated with hydroethidine (10 $\mu$M) and fluorescence quantitated by flow cytometry. *Bars,* ±SE; $P < 0.05$ *versus* the parental cell lines (*controls*), $n = 3$. *C,* after incubation with hydroethidine, cells were also examined by confocal laser scanning microscopy demonstrating that MIA PaCa-2 cells transfected with Ad*MnSOD* blocked the increase in hydroethidine fluorescence seen with treatment by dicumarol. *D,* cell growth. MIA PaCa-2 cells treated with dicumarol (100 $\mu$M) demonstrate reductions in cell growth compared with MIA PaCa-2 cells with no treatment. MIA PaCa-2 cells that had increased expression of MnSOD and were treated with dicumarol demonstrated growth similar to the parental cell line. Each point was determined in triplicate from the same culture. *, $P < 0.001$ *versus* MIA PaCa-2 cells (*controls*).

dicumarol (100 $\mu$M), and MIA PaCa-2 cells infected with Ad*MnSOD* and then treated with dicumarol (100 $\mu$M). Enforced expression of MnSOD with Ad*MnSOD* partially blocked the inhibition of cell growth from dicumarol treatment at 24 h (Fig. 4*D*).

## DISCUSSION

Our study demonstrates a potential role of $NQO_1$ in the growth of pancreatic cancer. $NQO_1$ was present in only very small amounts in normal pancreas and up-regulated in the pancreatic cancer cell lines. $NQO_1$, a flavoenzyme, catalyzes the two-electron reduction of quinones. This reaction then prevents the one-electron reduction of quinones by cytochrome P450 reductase and other flavoproteins that would result in redox cycling with generation of $O_2^{\cdot -}$ (7). This oxidoreductase electron transport system is a respiratory couple found in all of the eukaryotic cells. It functions as another system, in addition to utilization of NADH by mitochondria and by the pyruvate/lactate couple, for reoxidation of NADH derived from cellular metabolism to maintain the required $NAD^+$:NADH ratio to support cell viability (22). Our present study demonstrates that $NQO_1$ is up-regulated in pancreatic cancer cell lines, which is consistent with previous studies that have shown that expression of $NQO_1$ is up-regulated in tumors of the liver, lung, colon, breast, and pancreas compared with normal tissues of the same origin (19, 22). Additionally, in cells that lack mitochondria, activity of this plasma membrane oxidoreductase system is greatly up-regulated to support cell growth (30). Previous investigations have hypothesized that $NQO_1$ is up-regulated in various tumors to accommodate the needs of rapidly metabolizing cells to regenerate $NAD^+$ (31). $NQO_1$ has attracted interest over the years as an enzyme involved in detoxification of xenobiotics such as quinones and quinone-imines (14–16), and an enzyme associated with protection against mutagenesis and carcinogenesis (11–13). $NQO_1$ has also been characterized as being capable of generating antioxidant forms of ubiquinone and vitamin E during oxidative states, providing evidence that this enzyme may function as an antioxidant (9, 10).

Previous studies have demonstrated a specific growth-inhibitory effect of dicumarol in some tumor cell lines. Inhibition of $NQO_1$ by dicumarol is not from interference with vitamin K epoxide oxidoreductase or a previously unrecognized aspect of vitamin K metabolism, because addition of vitamin K does not impair the growth-inhibiting effect of dicumarol in melanoma cells (31). The growth-inhibitory effect of dicumarol may also be relatively specific for tumor cells, because proliferation of normal human airway myocytes was not affected (32). Indeed, our studies demonstrate that normal pancreas has little $NQO_1$ immunoreactive protein compared with the abundant amount of protein in the pancreatic cancer cell lines studied. Thus, the growth-inhibitory effect of dicumarol may not affect normal pancreas, whereas inhibition of $NQO_1$ by dicumarol

changes the malignant phenotype of pancreatic cancer by decreasing cell growth, plating efficiency, and growth in soft agar.

The role of $NQO_1$ in biological systems has been determined by the use of the competitive inhibitor dicumarol, which binds reversibly to the pyridine nucleotide binding site on $NQO_1$ and is competitive against pyridine nucleotide (33, 34). Dicumarol has been used as a component of the standard activity assay for $NQO_1$ for many years (20); however, it can inhibit many enzymes in addition to $NQO_1$ (35). Dicumarol is also extensively protein bound, which can complicate its use in cellular systems (36). Furthermore, the effective concentration of dicumarol that is required to inhibit $NQO_1$ depends on the efficiency of the second substrate or electron acceptor because of the competitive nature of dicumarol inhibition and the "ping-pong" kinetic mechanism of $NQO_1$ (37).

Our study also compliments the recent study from Li *et al.* (38) that demonstrated inhibition of NADPH oxidase with iodonium compounds including DPI, resulting in increased mitochondrial $O_2^{\cdot -}$ production leading to apoptosis. DPI, which inhibits flavoenzymes like $NQO_1$, increased ethidium fluorescence in HL-60 cells, and the DPI-induced generation of $O_2^{\cdot -}$ was reduced by overexpression of MnSOD. In our study, inhibition of $NQO_1$ increased hydroethidine fluorescence, and the dicumarol-induced generation of $O_2^{\cdot -}$ was also reduced by overexpression of MnSOD. Although previous studies in rat liver have demonstrated that the bulk of $NQO_1$ is located in the cytoplasm, lesser amounts are present in the mitochondria (39). The cellular distribution of $NQO_1$ in rapidly dividing tumor cells is variable (40). However, increasing mitochondrial superoxide production may prove to be a useful mechanism in treating cells that overexpress $NQO_1$.

The mechanisms involved in the growth-inhibitory effects of dicumarol may be different depending on the cell line studied. In our present study, dicumarol resulted in an increased intracellular burst of $O_2^{\cdot -}$ as measured by hydroethidine. In cells transiently transfected with the antioxidant MnSOD and then treated with dicumarol, $O_2^{\cdot -}$ levels were decreased compared with treatment with dicumarol alone, whereas cell growth was similar to the parental cell line suggesting that the increased intracellular generation of $O_2^{\cdot -}$ may be involved in the growth-inhibitory effects of dicumarol in pancreatic cancer cells. Brar *et al.* (31) have demonstrated a similar reduction in cell growth in a melanoma cell line treated with dicumarol. Malignant melanoma M1619 cells also demonstrate expression of $NQO_1$ by RT-PCR, and growth inhibition with dicumarol and other flavoenzyme inhibitors. However, in the melanoma cell line, measurement of $O_2^{\cdot -}$ by the cytochrome *c* assay suggested that the highest dose of dicumarol (250 $\mu$M) decreased $O_2^{\cdot -}$ generation. Our present study demonstrated that dicumarol (250 $\mu$M) did not affect cytochrome *c* reduction, lucigenin-enhanced chemiluminescence, or hydroethidine staining when compared with the parental cell line, but had the greatest effect in inhibition of *in vitro* cell growth. These differences may be explained in that the higher dose of dicumarol is extremely toxic to both the pancreatic and melanoma cell lines leading to overwhelming cell death. Also, there may be a different mechanism involved depending on the cellular compartment, which is affected by $NQO_1$ inhibition. Lower doses of dicumarol (100 $\mu$M) also did not change cytochrome *c* reduction or lucigenin-enhanced chemiluminescence, but increased hydroethidine staining, in a similar fashion as the nonspecific flavoenzyme inhibitor, DPI, which was also demonstrated by the study of Li *et al.* (38). Increased levels of hydroethidine staining (intracellular $O_2^{\cdot -}$), but not lucigenin-enhanced chemiluminescence (total $O_2^{\cdot -}$) or cytochrome *c* (extracellular $O_2^{\cdot -}$), suggests that in MIA PaCa-2 pancreatic cancer cells, inhibition of $NQO_1$ results in intracellular generation of $O_2^{\cdot -}$.

Adenocarincoma of the pancreas is resistant to almost all classes of chemotherapeutic drugs. Currently, the only active agent appears to be the DNA chain terminator gemcitabine (2′,2′-diflurodeoxycytidine), which results in an response rate of <20% (4). Even after curative resection, the 5-year survival rates achieved at specialized centers are <20%, and the majority of patients die of metastatic cancer recurrence (3). Other adjuvant treatments such as radiation therapy and chemotherapy have not improved long-term survival after resection. Thus, novel treatment strategies directed against this devastating malignancy are greatly needed.

In summary, $NQO_1$ is up-regulated in pancreatic cancer cell lines but absent in the normal human pancreas. Selective inhibition of $NQO_1$ with dicumarol alters the malignant phenotype MIA PaCa-2 pancreatic cancer cells by inhibiting cell growth, plating efficiency, and growth in soft agar. The mechanism involved in growth inhibition of pancreatic cancer by selective inhibition of $NQO_1$ appears to be an increased intracellular production of $O_2^{\cdot -}$. Both the increased intracellular production of $O_2^{\cdot -}$ and the growth inhibition by dicumarol are blunted with transfection of an adenoviral vector containing the cDNA for MnSOD. These mechanisms suggest that altering the intracellular redox environment of pancreatic cancer cells may be an effective strategy directed against pancreatic cancer.

## REFERENCES


1. Jemal, A., Thomas, A., Murray, T., Thun, M. Cancer statistics, 2002. CA Cancer J. Clin., *52:* 23–47, 2002.
2. Bramhall, S. R., Allum, W. H., Jones, A. G., Allwood, A., Cummins, C., Neoptolemos, J. P. Treatment and survival in 13,560 patients with pancreatic cancer, and incidence of the disease, in the epidemiological study. Br. J. Surg., *82:* 111–115, 1995.
3. Yeo, C. J., Cameron, J. L. Pancreatic cancer. Cur. Probl. Surg., *36:* 59–152, 1999.
4. Burris, H. A., Moore, M. J., Andersen, J., Green, M. R., Rothenber, M. I., Modiano, M. R., Cripps, M. C., Portenoy, R. K., Storniolo, A. M., Tarassoff, P., Nelson, R., Dorr, F. A., Stephens, C. D., and von Hoff, D. D. Improvements in survival and clinical benefit with gemcitabine as first-line therapy for patients with advanced pancreatic cancer: a randomized trial. J. Clin. Oncol., *15:* 2403–2413, 1997.
5. Jessup, J. M., Steele, G., Mayer, R. J., *et al.* Neoadjuvant therapy for unresectable pancreatic adenocarcinoma. Arch. Surg., *128:* 559–564, 1993.
6. White, R., Lee, C., Anscher, M., *et al.* Preoperative chemoradiation for patients with locally advanced sdenocarcinoma of the pancreas. Ann. Surg. Oncol., *6:* 38–45, 1999.
7. Ernster L. DT-diaphorase. Methods Enzymol., *10:* 309–317, 1967.
8. Sun, I. L., Sun, E. E., Crane, F. L., Morre, D. J., Lindgren, A., and Low, H. Requirement for coenzyme Q in plasma membrane electron transport. Proc. Natl. Acad. Sci. USA, *89:* 11126–11130, 1992.
9. Beyer, R. E., Segura-Aguilar, J., DiBernardo, S., Cavazzoni, M., Fato, R., Fiorentini, D., Galli, M., Setti, M., Landi, L., and Lenaz, G. The role of DT-diaphorase in the maintenance of the reduced antioxidant form of coenzyme Q in membrane systems. Proc. Natl. Acad. Sci. USA, *93:* 2528–2532, 1996.
10. Siegel, D., Bolton, E. M., Burr, J. A., Liebler, D. C., and Ross, D. The reduction of α-tocopherolquinone by human NAD(P)H:quinone oxidoreductase: the role of α-tocopherol hydroquinone as a cellular antioxidant. Mol. Pharmacol., *52:* 300–305, 1997.
11. Benson, A. M., Hunkler, M. G., and Talalay, P. Increase of NAD(P)H:quinone reductase by dietary antioxidants: possible role in protection against carcinogenesis and toxicity. Proc. Nat. Acad. Sci. USA., *77:* 5216–5220, 1980.
12. Talalay, P., DeLong, M. G., and Prochaska, H. J. Identification of a common chemical signal regulating the induction of enzymes that protect against chemical carcinogenesis. Proc. Natl. Acad. Sci. USA, *85:* 8261–8265, 1988.
13. Trush, M. A., Twerdok, L. E., Rembish, S. J., Zhu, H., and Li, Y. B. Analysis of target cell susceptibility as a basis for the development of a chemoprotective strategy against benzene-induced hematotoxicities. Environ. Health Perspect., *104*(Suppl. 6)*:* 1227–1234, 1996.
14. Chesis, P. L., Levin, D. E., Smith, M. T., Ernster, L., and Ames, B. N. Mutagenicity of quinines: pathways of metabolic activation and detoxification. Proc. Nat. Acad. Sci. USA., *81:* 1696–1700, 1984.
15. Lind, C., Hochstein, P., and Ernster, L. DT-Diaphorase as a quinone reductase: a cellular control device against semiquinone and superoxide radical formation. Arch. Biochem. Biophys., *216:* 178–185, 1982.
16. Thor, H., Smith, M. T., Hartzell, P., Bellomo, G., Jewell, S. A., and Orrenius, S. The metabolism of menadione (2-methyl-1,4-naphthoquinone) by isolated hepatocytes. A study of the implication of oxidative stress in intact cells. J. Biol. Chem., *257:* 12419–12425, 1982.
17. Siegel, D., and Ross, D. Immunodetection of NAD(P)H:quinone oxidoreductase 1 (NQO1) in human tissues. Free Rad. Biol. Med., *29:* 246–253, 2000.
18. Malkinson, A. M., Siegel, D., Forrest, G. L., Gazdar, A. F., Oie, H. K., Chan, D. C., Bunn, P. A., Mabry, M., Dykes, D. J., Harrsion, S. D., and Ross, D. Elevated

DT-diaphorase activity and messenger RNA content in human non-small cell lung carcinoma: relationship to the response of lung tumor xenografts to mitomycin C. Cancer Res., *52:* 4752–4757, 1992.
19. Logsdon, C. D., Simeone, D. M., Binkley, C., Arumugam, T., Greenson, J. K., Giordano, T. J., Misek, D. E., and Hanash, S. Molecular profiling of pancreatic adenocarcinoma and chronic pancreatitis identifies multiple genes differentially regulated in pancreatic cancer. Cancer Res., *63:* 2649–2657, 2003.
20. O'Donnell, V. B., Smith, G. C. M., and Jones, O. T. G. Involvement of phenyl radicals in iodonium compound inhibition of flavoenzymes. Mol. Pharmacol., *46:* 778–786, 1994.
21. Edwards, Y. H., Potter, J., and Hopkinson, D. A. Human FAD-dependent NADPH diaphorase. Biochem. J., *187:* 429–436, 1980.
22. Belinskiy, M., and Jaiswal, A. K. NADPH:quinone oxidoreductase$_1$ (DT-diaphorase) expression in normal and tumor tissues. Cancer Metastasis Rev., *12:* 103–117, 1993.
23. Li, J. J., Oberley, L. W., St. Clair, D. K., Ridnour, L. A., and Oberley, T. D. Phenotypic changes induced in human breast cancer cells by overexpression of manganese-containing superoxide dismutase. Oncogene, *10:* 1989–2000, 1995.
24. Gasdaska, P. Y., Fisher, H., and Powis, G. An alternatively spliced form of $NQO_1$ (DT-diaphorase) messenger RNA lacking the putative quinone substrate binding site is present in human normal and tumor tissues. Cancer Res., *55:* 2542–2547, 1995.
25. Fitzsimmons, S. A., Workman, P., Grever, M., Paull, K., Camalier, R., and Lewis, A. D. Reductase enzyme expression across the National Cancer Institute tumor cell line panel: correlation with sensitivity to mitomycin C and EO9. J. Natl. Cancer Inst., *88:* 259–269, 1996.
26. Cullen, J. J., Weydert, C. J., Hinkhouse, M. M., Domann, F. E., Spitz, D. R., and Oberley, L. W. The role of manganese superoxide dismutase in the growth of pancreatic adenocarcinoma. Cancer Res., *63:* 1297–1303, 2003.
27. Cullen, J. J., Mitros, F. A., and Oberley, L. W. Expression of antioxidant enzymes in diseases of the human pancreas: another link between chronic pancreatitis and pancreatic cancer. Pancreas, *26:* 23–27, 2003.
28. Oberley, T. D., Oberley, L. W., Slattery, A. F., Lauchner, L. J., and Elwell, J. H. Immunohistochemical localization of antioxidant enzymes in adult Syrian hamster tissues and during kidney development. Am. J. Pathol., *137:* 199–214, 1990.
29. Misra, V., Klamut, H. J., and Rauth, A. M. Expression of the prodrug-activating enzyme DT-diaphorase *via* Ad5 delivery to human colon carcinoma cells *in vitro*. Cancer Gene Ther., *9:* 209–217, 2002.
30. Larm, J. A., Vaillant, F., Linnane, A. W., and Lawen, A. Up-regulation of the plasma membrane oxidoreductase as a prerequisite for the viability of human Namalwa $\rho^{o}$ cells. J. Biol. Chem., *269:* 30097–30100, 1994.
31. Brar, S. S., Kennedy, T. P., Whorton, A. R., Sturrock, A. B., Huecksteadt, T. P., Ghio, A. J., and Hoidal, J. R. Reactive oxygen species from NAD(P)H: quinone oxidoreductase constitutively activate NF-$\kappa$ B in malignant melanoma cells. Am. J. Physiol., *280:* C659–C676, 2001.
32. Brar, D. D., Kennedy, T. P., Whorton, A. R., Murphy, T. M., Chitano, P., and Hoidal, J. R. Requirement for reactive oxygen species in serum-induced and platelet-derived growth factor-induced growth of airway smooth muscle. J. Bio. Chem., *274:* 20017–20026, 1999.
33. Hollander, P., and Ernster, L. Studies on the reaction mechanism of DT diaphorase. Action of dead-end inhibitors and effects of phospholipids. Arch. Biochem. Biophys., *169:* 560–567, 1975.
34. Josoda, S., Nakamura, W., and Hayashi, K. Properties and reaction mechanisms of DT diaphorase from rat liver. J. Biol. Chem., *249:* 6416–6423, 1974.
35. Ross, D., Siegel, D., Beall, H., Prakash, A. S., Mulcahy, R. T., and Gibson, N. W. DT-diaphorase in activation and detoxification of quinones. Bioreductive activation of mitomycin C. Cancer Metastasis Rev., *12:* 83–101, 1993.
36. Hulse, M., Feldman, S., and Bruckner, J. V. Effect of blood sampling schedules on protein drug binding in the rat. J. Pharmacol. Exp. Ther., *218:* 416–420, 1981.
37. Preusch, P. C., Siegel, D., Givson, N. W., and Ross, D. A note on the inhibition of DT-diaphorase by dicoumarol. Free Radic. Biol. Med., *11:* 77–80, 1991.
38. Li, N., Ragheb, K., Lawler, G., Sturgis, J., Rajwa, B., Melendez, J. A., and Robinson, J. P. DPI induces mitochondrial superoxide-mediated apoptosis Free Radic. Biol. Med. *34:* 465–477, 2003.
39. Edlund, C., Elhammer, A., and Dallner, G. Distribution of newly synthesized DT-diaphorase in rat liver. Biosci. Rep., *2:* 861–865, 1982.
40. Winski, S. L., Koutalos, Y., Bentley, D. L., and Ross, D. Subcellular localization of NAD(P)H:quinone oxidoreductase 1 in human cancer cells. Cancer Res., *62:* 1420–1424, 2002.